المحفل العلمي الدولي

ARID Journals

ARID International Journal for Science and Technology (AIJST)
ISSN: 2662-009X

Journal home page: http://arid.my/j/aijst

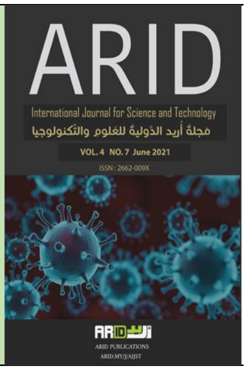

مَجلةُ أُريد الدَّوليةُ للعُلومِ والتِّكنولوجيا

العدد 7 ، المجلد 4 ، حزيران 2021 م

Evaluation of the Crack Model of V Type Longitudinal Ribs on Orthotropic Deck Using Finite Element Analysis

Fatih Alemdar

Department of Civil Engineering, Civil Engineering Faculty, Yıldız Technical University, Davutpaşa, Esenler, Istanbul 34220, Turkey.

تقييم نموذج التصدع للأضلاع الطولية من النوع V على سطح تقويمي باستخدام نموذج تحليل العناصر المحدودة

فاتح علم دار

قسم الهندسة المدنية، كلية الهندسة المدنية، جامعة يلدز التقنية-اسطنبول - تركيا

falemdar@yildiz.edu.tr
arid.my/0004-0654
https://doi.org/10.36772/arid.aijst.2021.474

ARTICLE INFO

Article history:
Received 28/01/2021
Received in revised form 16/03/2021
Accepted 19/05/2021
Available online 15/06/2021
https://doi.org/10.36772/arid.aijst.2021.474

Abstract

The long span orthotropic bridge decks applied around the world are used with open or closed cross-sectional longitudinal ribs placed below the steel deck to increase the strength of the deck. Fatigue cracks are developed in the longitudinal ribs due to traffic loadings. In this study, v type of longitudinal rib cross-sections are modelled and the stresses for the rib are evaluated under tire load loading using finite element analysis. Longitudinal ribs are used for long span steel bridges. The aim of this study is to compare the fatigue crack path of the longitudinal rib on a real bridge with the stress pattern in the finite element model.

Keywords: Finite Element, Orthotropic deck, Fatigue crack stop hole, Steel bridges, Longitudinal rib

الملخص

تُستخدم أسـطح الجسـر التقويميـة طويلـة المـدى المنفـذة حـول العـالم مـع أضـلاع طوليـة مقطعيـة مفتوحـة أو مغلقـة والموضـوعة أسـفل السـطح الفـولاذي لزيـادة قوتـه ومتانتـه. حيـث طـورت شـقوق الإجهـاد فـي الأضـلاع الطوليـة بسـبب الأحمـال المروريـة الثقيلـة. حيـث تـم، فـي هـذه الدراسـة، نمذجـة النـوع الخـامس مـن المقـاطع العرضـية للأضـلاع الطوليـة وتقيـيم ضـغوط الضـلع تحـت حمـل إطـارات المركبـات وذلـك باسـتخدام مقيـاس تحليـل العناصـر المحـدودة. وقـد اسـتخدمت الأضـلاع الطوليـة للجسـور الفولاذيـة الطويلـة. إن الهـدف مـن هـذه الدراسـة هـو مقارنـة مسـار شـق الإجهـاد في الضلع الطولي على جسر حقيقي مع نمط الإجهاد في نموذج تحليل العناصر المحدودة.

كلمات مفتاحية: عنصر محدود، سطح متعامد، فتحة توقف صدع الاجهاد، جسور فولاذية، ضلع طولي.

1. Introduction

Longitudinal ribs constructed in the steel bridges are divided into two categories: (a) open cross-sectional ribs and (b) closed form longitudinal ribs. The strength of the open form longitudinal ribs are less than that of the closed form ribs and thus open form ribs are not utilized in practice (Fig. 1). Closed form longitudinal ribs generally consist of triangular and trapezoidal cross sections. The triangular longitudinal ribs were usually utilized in the steel bridges constructed before 1980s. Trapezoidal longitudinal ribs have been built in the bridges designed after 1980s. The main reason can be easier construction of the trapezoidal ribs than that of the triangular ribs. The secondary reasons may be considered as the top width of the trapezoidal rib is larger and less ribs are required for construction of bridges and thus labour is reduced.

The experimental studies on triangular longitudinal ribs are very few. Generally, steel bridge decks were modelled using finite element method (FEM) and the stresses at the critical regions were obtained. Stresses along the bridge decks were determined using different analysis programs [1-22]. Therefore; realistic information about the behaviour of the bridge decks under the loadings and the crack regions can be obtained. However, the stresses found by the analysis cannot reflect the real situations due to the assumptions done in the simulations. The results are getting closer to the real numbers depending on the assumptions made in the program and the formulae used in the analysis. Therefore; the finite element method is a well-recognized method in the World due to giving closer results to the real values.

Empirical equations were derived to calculate the construction expense of a bridge depending on the thickness of the plate and the minimum thickness of the plate to be used in the bridge was obtained [16]. This study was performed on the bridges having less traffic loads and thus it may not be utilized for the bridges having long span and heavy traffic loads.

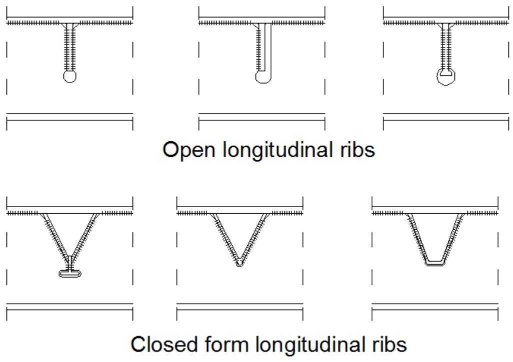

Figure(1): Steel orthotropic deck longitudinal rib types

2. Objectives

This study aims to investigate longitudinal rib body and diaphragm plate cracks modelling. The connection between the crack paths along the ribs on a real bridge and the stress distribution on the FE model is studied. The cracks on the rib – rib connection and rib – diaphragm plate connection are separately modelled. In the diaphragm plates cracks repaired with using different drilled holes diameter are evaluated. In addition, a parametric study is performed by changing the length of the cracks occurred downward at the region where the diaphragm plate and side of the rib are connected.

3. Details of the Longitudinal Ribs

Triangular longitudinal rib examined analytically in this study is shown in Fig. 3. The cross-sections of the rib studied here are the details of existence ribs used in Bosporus bridge in Istanbul [23, 24]. The distance between two ribs is 300 mm. The connection plate of the ribs is modelled the same for each rib detail. The length of the lap splice is modelled as 15 mm and the distance between the ribs is defined as 150 mm. The connections are welded through ribs and the sides of the connection plate. The welding used to connect the ribs to the upper plate is not taken into account in the analysis. The depth of the ribs is defined as 1500 mm the height of the diaphragm is 750 mm selected so that no stress concentration could occur under the rib. Diaphragm is welded both on the sides of the rib at the centre of the rib and top plate and defined as fix bottom side of the diaphragm plate. The perpendicular edge of the diaphragm is not constraint which are free to move and the thickness is 8 mm (Fig. 4).

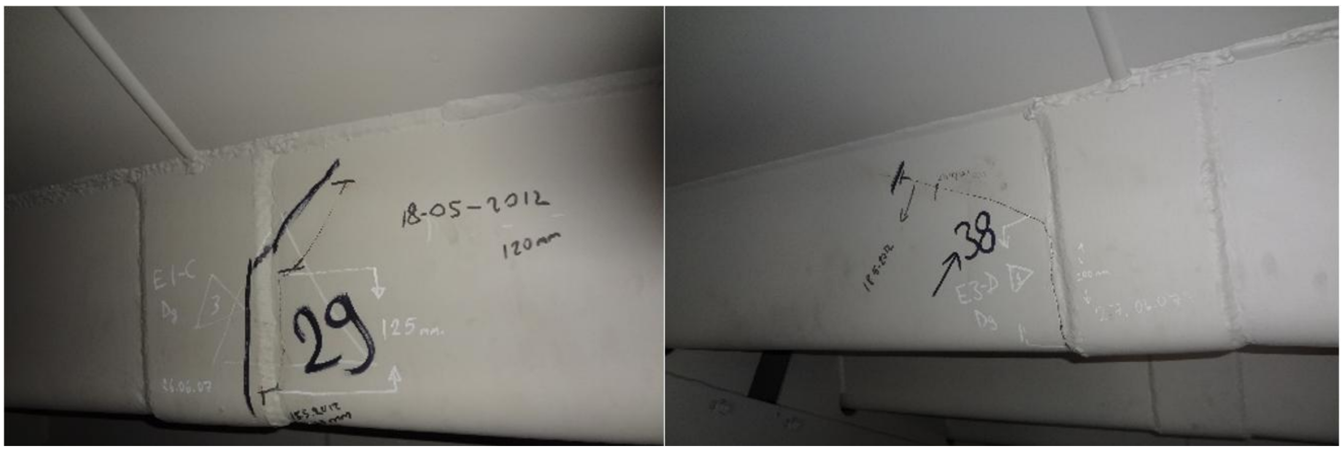

Figure(2): Triangular longitudinal rib to rib connection region fatigue cracks.

Figure(3): Triangular longitudinal ribs to diaphragm plate region fatigue cracks.

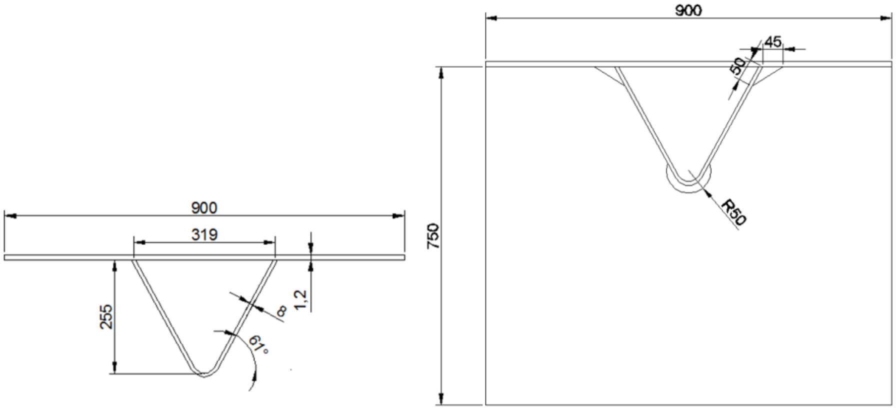

Figure(4): Triangular rib and diaphragm plate details (dimensions in mm).

4. General crack path of the ribs

Cracks are generally occurred at the connection areas of the ribs. These areas are the regions where the ribs are connected side by side and the point ribs are connected to the diaphragm plates. Cracks occurred at the connection region of the ribs are shown in Fig. 2. The second type of the cracks is shown Fig. 3. The third type of cracks develops downward at the welds between the diaphragm plate and the longitudinal rib (Fig.5b). These three types of cracks are investigated in this study.

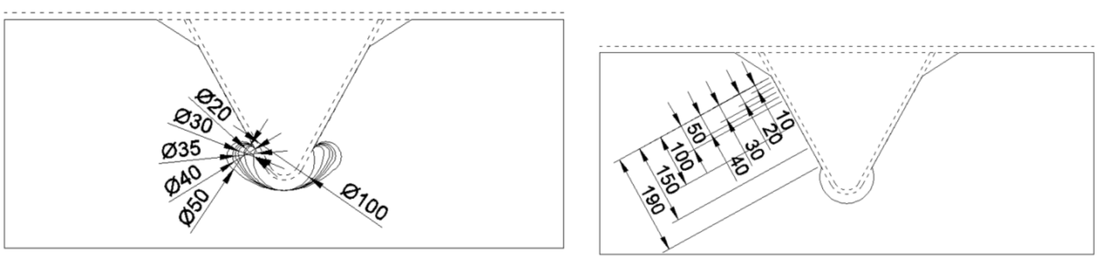

Figure(5): Diaphragm plate bottom fatigue crack repair with different hole diameter and crack between diaphragm plate and rib different crack length details (dimensions in mm).

5. Finite Element Modelling of the Ribs

In this study, the longitudinal rib and the components of the deck used in orthotropic bridge decks and a part of a tire (275/70 R22.5) used for transportation buses are modelled using a finite element program. The surface area of the tire gets larger when the axial load from the transportation vehicle is applied, thus larger surfaces area is accounted in the FE analysis. The width of the model is defined as the depth of the longitudinal rib. The longitudinal rib in this study consists of triangular cross-section.

The longitudinal ribs, the upper plate and the tire are defined using steel material. The young modulus and poison ratio are given as 210 GPa and 0.1, respectively. The road is modelled using asphalt material and the young modulus and poison ratio are 2.5 GPa and 0.3 respectively. The reason of modelling the tire with steel material is that the most important part of the analysis is to evaluate the longitudinal rib and not to have any unexpected deformations in the tire. All the materials in the finite element model are defined using solid homogenous material type. The boundary conditions of the longitudinal rib and the upper plate at each end location are constrained in displacement and released in rotation. The connections between the asphalt and the upper plate, and the longitudinal rib and the plate are modelled using tie constraint in the analysis.

The thicknesses of the plates are 8 mm and 12 mm for the longitudinal rib and the upper plate respectively. The thickness of the asphalt is taken as 33 mm. The weld thickness in the connection region is defined as 5.5 mm. An 8 mm thick plate is used to connect the longitudinal ribs and the length of the lap splice is defined as 15 mm. The connection plate is taken as 180 mm long. The interaction between the connection plate, the weld and the longitudinal rib is chosen as tie constraint to provide full connection. The thickness of the diaphragm plate is 8 mm and height of the plate is 750 mm diaphragm plate and longitudinal rib connect with tie constraint and weld between diaphragm plate and rib is not defined.

The mesh size for the whole finite element model is around 10 mm and an 8-node linear brick element (C3D8R) is defined for the mesh element as shown in (Fig. 6). The axial load of 100 kN concentrated force of is applied at the centre of the tire. This load is taken from Turkish bridge code weight hos H30S24 truck having 240 kN axle load. There are 4 tires at each axle and thus a load of a tire is 60 kN. The normal load from a tire is accounted as 90 kN when the dynamic amplification factor is taken as 1.5.

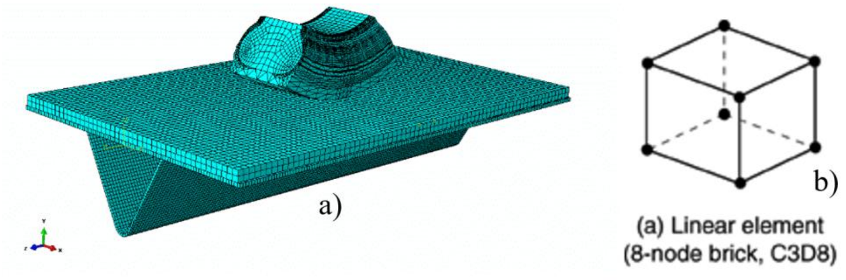

Figure(6): Finite element assembly mesh (a) and element type (b)

In this part of the analysis, longitudinal ribs are continuous under the bridge deck. The stresses on the longitudinal rib of a bridge deck due to tire loading are examined along the deck and away from the support regions of the bridge. The finite element model is built as if the tire passes in the middle of the longitudinal rib (Fig. 7). Hard contact interaction and friction are defined between the tire and the asphalt surface.

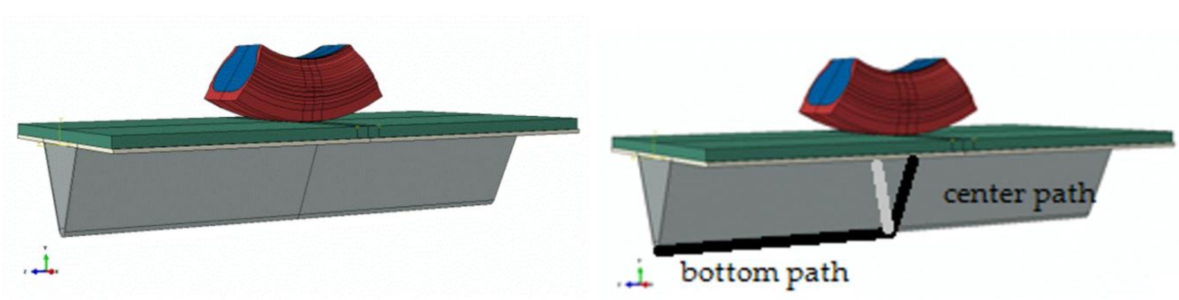

Figure(7): Finite element modelling continuous rib cross-sections and bottom and center paths

The connection region of the longitudinal ribs is also considered in this study. This region is generally constructed 1 m away from one end of the sector plate under the bridge deck for the real bridges. A finite element model of the connection plate and the weld to be used to combine the upper plate and the longitudinal rib is created. The thickness of the weld is chosen as 5.5 mm and applied around the thickness of the connection plate as a triangular welding. The lap splice of the connection plate on the ribs is 15 mm and the length of the plate is 180 mm (Fig. 8). Full interactions (tie constraint) between the plate and the weld and between the weld and the longitudinal rib are provided.

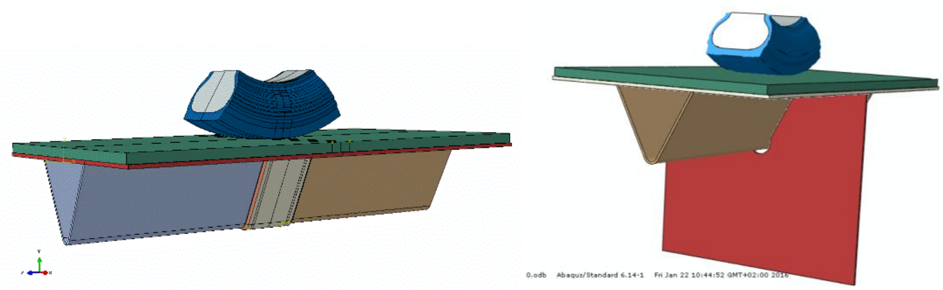

Figure(8): Finite element modelling rib connection area and diaphragm plate with continuous longitudinal rib

6. Parametric Analysis of the Ribs

The maximum principal stresses and the maximum deformations of the triangular longitudinal ribs are evaluated. The stress and the deformation contours along the vertical line perpendicular to the tire axis are shown in Fig. 9. In the model continuous rib, rib to rib connection region, and rib with diaphragm plate the maximum principal stress as seen in Fig. 9.

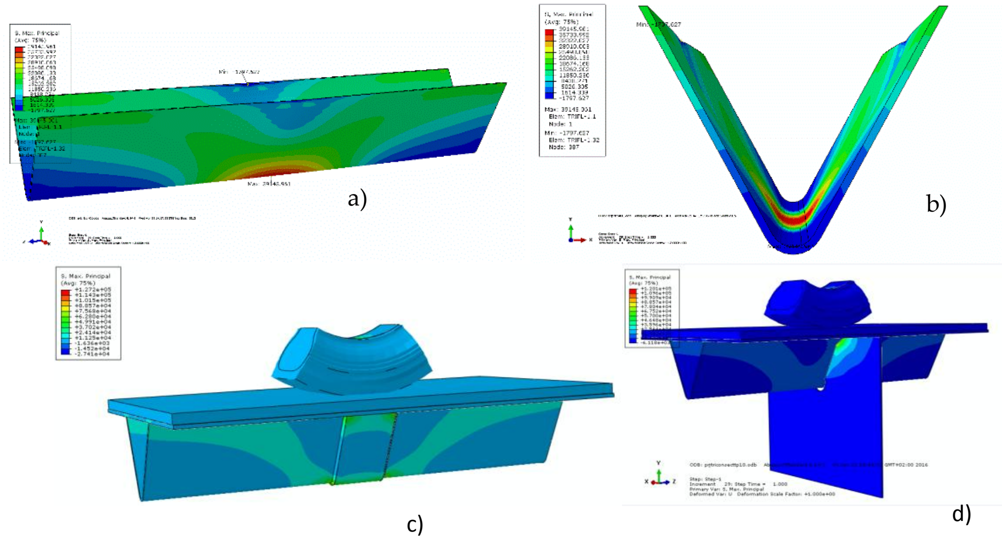

Figure(9): Max. Principal stress contours in the continuous rib (a) section view (b), and on the connection area (c) diaphragm plate with longitudinal rib (d)

6.1 Effect of Tire position on the ribs

The tire position is changed along the centre of the rib in this part of the analysis. The maximum principal stresses on the centre axis of the rib and on the longitudinal axis of the continuous rib are obtained according to the position of the tire and shown in the Fig. 10-11. The aim of the analysis is to examine the location of the tire since the tire does not always affect an orthotropic deck on the centre of the rib. The position of the tire was defined as 0, 50, 100, 150, 200, 250 mm where zero shows the centre of the rib and 250 mm shows the furthest location from the centre. The stresses on the centre line (centre path) of the longitudinal rib are illustrated in Fig. 10-11. In the FE models, only one rib with a specified length (1500 mm) was considered and there was no interaction defined from on the rib.

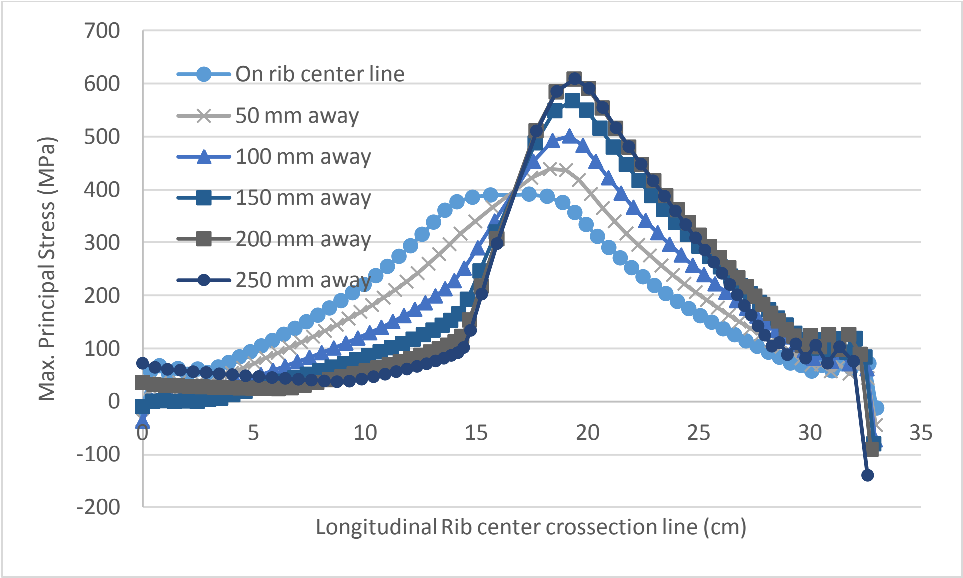

Figure(10): Longitudinal rib cross-section on the centre of the model

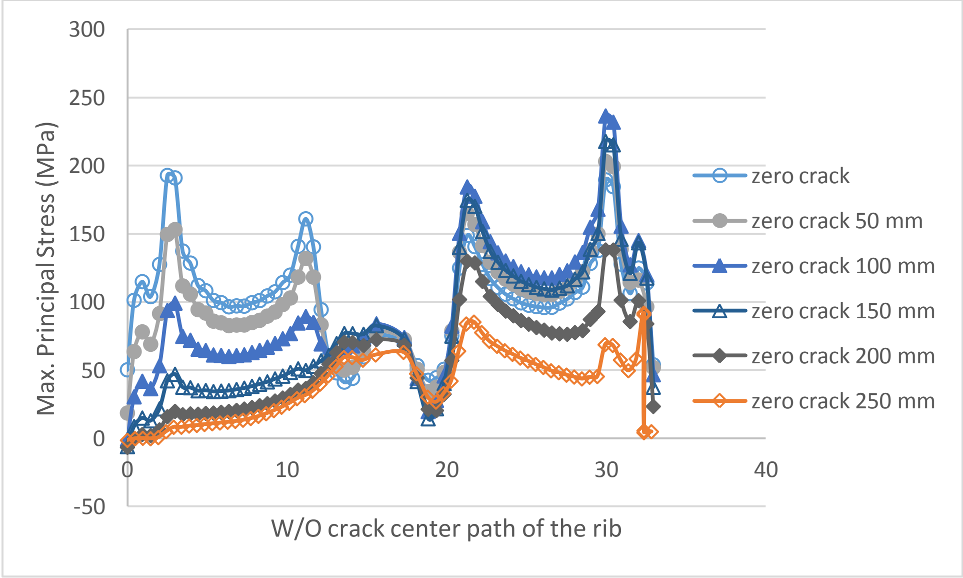

Figure(11): Longitudinal rib cross-section on the center of the model with diaphragm plate

6.2 Effect of crack repair with hole on the diaphragm plate

In this part of the analysis, the fatigue cracks at the region where the longitudinal ribs reach to the diaphragm plates are evaluated. The diameter of the drilled hole at the bottom of the ribs is changed to reduce the stress on the crack paths on the diaphragm plate. The diameter of the drilled hole is chosen between 20 mm - 50 mm (Fig.5a). The stress distribution along the centre path is shown in Fig. 12 and the stress distribution along the circumference length of the drilled hole is shown Fig. 13

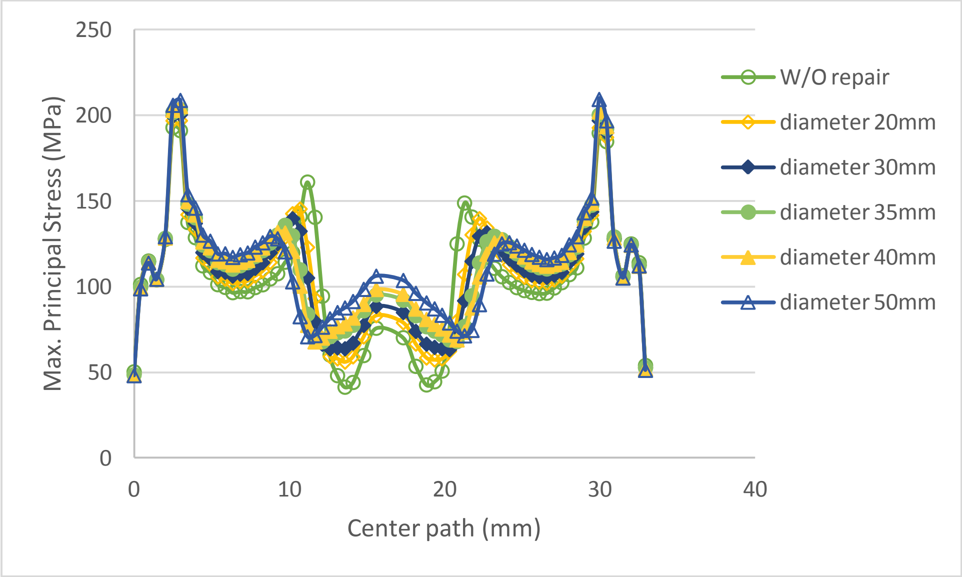

Figure(12): Longitudinal rib cross-section on the center of the model with diaphragm plate

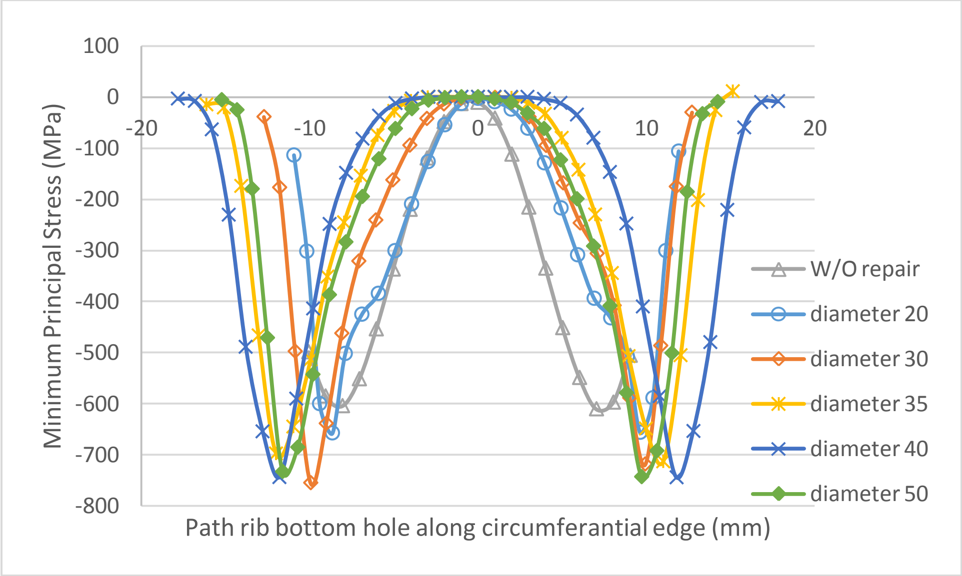

Figure(13): Longitudinal rib cross-section on the center of the model with diaphragm plate

6.3 Effect of crack length between diaphragm plate and longitudinal rib

The crack length along the welds between the diaphragm plate and the longitudinal rib altered from 10 mm to 190 mm in order to evaluate the effect of the crack length on one side of the rib. The cracks defined as leaving 1 mm space between the diaphragm plate and the rib on the diaphragm plate (Fig.5b). The stress distribution for different crack length is shown in Figure 14.

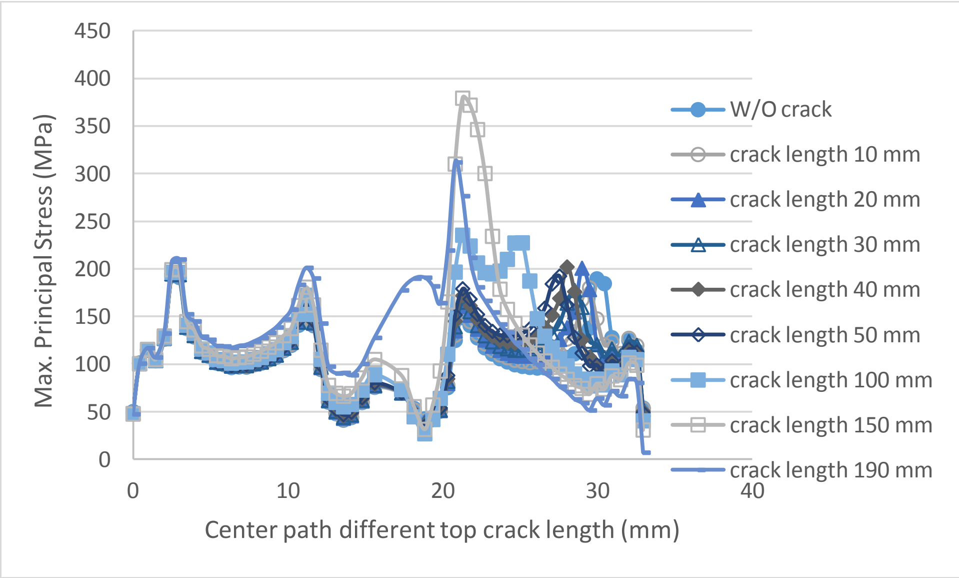

Figure(14): Longitudinal rib cross-section on the center of the model with diaphragm plate

7. Conclusions

The conclusion below are obtained from the FE analysis results.

- The stresses on the ribs are calculated under the maximum tire loading (100 kN) which is considered as the maximum load of one tire when the truck is fully loaded. The stress are higher away from the connection region along the bottom path of the rib for the model with connection plate when the tire is the centre position. However, the stresses on the welds around the connection plate are concentrated as shown in Fig 10. This results explains where the cracks start to grow as also shown in the Fig. 2. These findings are in line with the real situation.

- There is no difference obtained in the stress along the longitudinal axis of the rib when the position of the tire is changed. However, the maximum principal stresses occurred at the bottom point path and as well as on the bottom path of the rib when cross-sectional stresses are evaluated. The maximum stresses occur away from the centre of the rib as shown Fig. 10.
- The maximum stress values obtained in the cross-section of the rib coincides when the tire is 200 and 250 mm from centre. It can be concluded that the stress distribution may be obtained as the tire is 100 or 150 mm away from the centre since the effect of the length of the rib and the interaction between other ribs are excluded in the analysis. The maximum stress obtained when the tire is 150 mm away from the centre line is 1.16 times higher than the stress found in the analysis with the tire on the centre (Fig. 11). It may be observed that the fatigue cracks start to occur to the closed side of bottom of the rib. Tire position may effect to the maximum principal stress on the rib %22 higher depend on the centre loading.
- The maximum stress on the ribs when the crack on the diaphragm plate is repaired with different drilled hole diameter did not change (Fig. 12). Moreover, the maximum stresses along circumferential path increased comparing to without drilled hole. It is concluded that this repair method does not alleviate the stress concentration around the crack location. Especially, the ratio of the diameter of the drilled hole to the diameter of the arc at the bottom of the ribs is greater than 80% the stress concentration is growing around the drilled hole (Fig.13).
- The highest max principal stress occurred on diaphragm plate and ribs connection region when crack reached 150 mm long (Fig. 14). It is shown that

the crack length increases rapidly at this point. The maximum stress is doubled up when the crack length is 150 mm comparing to the maximum stress with no crack in the connection.

List of abbreviations:

FEM : Finite Element Method

FE : Finite Element

kN : Kilo Newton

FE model : Finite Element Model

GPa : Giga Pascal (kN/mm^2)

References

1. Z.X. Li, T.H.T. Chan, and T.Q. Zhou, *Accumulative damage near crack tip for welded bridge members: fatigue life determination.* Theoretical and Applied Fracture Mechanics, 2005. **43**(2): p. 245-260.
2. M. Aygül, M. Bokesjö, M. Heshmati, and M. Al-Emrani, *A comparative study of different fatigue failure assessments of welded bridge details.* International Journal of Fatigue, 2013. **49**(0): p. 62-72.
3. H.-T. Nguyen, Q.-T. Chu, and S.-E. Kim, *Fatigue analysis of a pre-fabricated orthotropic steel deck for light-weight vehicles.* Journal of Constructional Steel Research, 2011. **67**(4): p. 647-655.
4. S. Teixeira de Freitas, H. Kolstein, and F. Bijlaard, *Fatigue behavior of bonded and sandwich systems for strengthening orthotropic bridge decks.* Composite Structures, 2013. **97**(0): p. 117-128.
5. Z.G. Xiao, K. Yamada, J. Inoue, and K. Yamaguchi, *Fatigue cracks in longitudinal ribs of steel orthotropic deck.* International Journal of Fatigue, 2006. **28**(4): p. 409-416.
6. C. Miki, *Fatigue damage in orthotropic steel bridge decks and retrofit works.* International Journal of Steel Structures, 2006. **6**(4): p. 255-267.
7. Z.X. Li, T.H.T. Chan, and J.M. Ko, *Fatigue damage model for bridge under traffic loading: application made to Tsing Ma Bridge.* Theoretical and Applied Fracture Mechanics, 2001. **35**(1): p. 81-91.
8. B.N. Kaan, F. Alemdar, C.R. Bennett, A. Matamoros, R. Barrett-Gonzalez, and S. Rolfe, *Fatigue enhancement of welded details in steel bridges using CFRP overlay elements.* Journal of Composites for Construction, 2011. **16**(2): p. 138-149.
9. R.C. Battista, M.S. Pfeil, and E.M.L. Carvalho, *Fatigue life estimates for a slender orthotropic steel deck.* Journal of Constructional Steel Research, 2008. **64**(1): p. 134-143.
10. L. Frýba and L. Gajdoš, *Fatigue properties of orthotropic decks on railway bridges.* Engineering Structures, 1999. **21**(7): p. 639-652.
11. Z.-G. Xiao, T. Chen, and X.-L. Zhao, *Fatigue strength evaluation of transverse fillet welded joints subjected to bending loads.* International Journal of Fatigue, 2012. **38**(0): p. 57-64.
12. K. Kiss and L. Dunai, *Fracture mechanics based fatigue analysis of steel bridge decks by two-level cracked models.* Computers & Structures, 2002. **80**(27–30): p. 2321-2331.
13. F. Alemdar, A.B. Matamoros, C.R. Bennett, R. Barrett-Gonzalez, and S.T. Rolfe. *Improved method for bonding CFRP overlays to steel for fatigue repair*. in *Proc., ASCE/SEI Structures Congress*. 2011.
14. L. Frýba and S. Urushadze, *Improvement of fatigue properties of orthotropic decks.* Engineering Structures, 2011. **33**(4): p. 1166-1169.
15. M. Aygül, M. Al-Emrani, and S. Urushadze, *Modelling and fatigue life assessment of orthotropic bridge deck details using FEM.* International Journal of Fatigue, 2012. **40**(0): p. 129-142.
16. F. Alemdar, *Repair of bridge steel girders damaged by distortion-induced fatigue*. 2011, The University of Kansas.
17. F. Alemdar, D. Nagati, A. Matamoros, C. Bennett, and S. Rolfe, *Repairing Distortion-Induced Fatigue Cracks in Steel Bridge Girders Using Angles-with-*

Plate Retrofit Technique. I: Physical Simulations. Journal of Structural Engineering, 2013.

18. F. Alemdar, T. Overman, A. Matamoros, C. Bennett, and S. Rolfe, *Repairing Distortion-Induced Fatigue Cracks in Steel Bridge Girders Using Angles-with-Plate Retrofit Technique. II: Computer Simulations.* Journal of Structural Engineering, 2013.
19. M.A. Wahab and M.S. Alam, *The significance of weld imperfections and surface peening on fatigue crack propagation life of butt-welded joints.* Journal of Materials Processing Technology, 2004. **153–154**(0): p. 931-937.
20. Z.-G. Xiao, K. Yamada, S. Ya, and X.-L. Zhao, *Stress analyses and fatigue evaluation of rib-to-deck joints in steel orthotropic decks.* International Journal of Fatigue, 2008. **30**(8): p. 1387-1397.
21. J. Sim and H. Oh, *Structural behavior of strengthened bridge deck specimens under fatigue loading.* Engineering Structures, 2004. **26**(14): p. 2219-2230.
22. F. Alemdar, A. Matamoros, C. Bennett, R. Barrett-Gonzalez, and S.T. Rolfe, *Use of CFRP overlays to strengthen welded connections under fatigue loading.* Journal of Bridge Engineering, 2011. **17**(3): p. 420-431.
23. F. Alemdar, *Evaluation of the Performance of Stress Measures for Longitudinal Ribs on Orthotropic deck Using Finite Element Analysis.* 2015.
24. H.S. Celasun, *Asma Köprüler*. Vol. 160. 1981: İDMM Academy. 326.